

Atmospheric Research for Adaptive Optics

L. A. Bolbasova^{a, *} and V. P. Lukin^{a, **}

^a V.E. Zuev Institute of Atmospheric Optics, Siberian Branch, Russian Academy of Sciences, Tomsk, 634055 Russia

*e-mail: sla@iao.ru

**e-mail: lukin@iao.ru

Received February 8, 2021; revised February 8, 2021; accepted March 9, 2021

Abstract—Adaptive optics (AO) systems are an essential part of large astronomical telescopes and laser complexes operating through the atmosphere. Each AO system is individually designed; the requirements for the components and the performance of an AO system are determined by the intensity and distribution of turbulent fluctuations of the air refractive index over the radiation propagation path. In this work, we review the techniques and instruments for measuring and forecasting atmospheric conditions for AO, including devices and techniques developed at the Institute of Atmospheric Optics, Siberian Branch, Russian Academy of Sciences. The basic principles of atmospheric AO and the related atmospheric parameters are briefly described. Particular attention is paid to the parameter used for the estimation of capabilities of AO systems, i.e., the wind speed at a level of 200 hPa. The comparison with the data from foreign astronomical observatories is carried out. The necessity for atmospheric research for large Russian astronomical observatories is discussed.

Keywords: adaptive optics, atmospheric optical turbulence, astronomical seeing, measurement technique

DOI: 10.1134/S1024856022030022

INTRODUCTION

Random inhomogeneities of the refractive index of the Earth's atmosphere distort propagating optical radiation, which is shown in jitter, scintillation, and degradation of optical images and laser beams. Adaptive optics systems are designed for real-time compensation for these effects.

In 1953, Babcock [1] suggested using controllable optical feedback components to compensate for turbulent atmospheric distortions. In 1957, Linnik studied the possibility of eliminating distortions induced by atmospheric turbulence [2]. He suggested a telescope design with a composite mirror with moving elements, which allowed real-time wavefront adjustment. That idea supported by modern technologies gradually evolved into an independent branch of physical optics – adaptive optics (AO).

The main aim of adaptive optics is the development of techniques and instruments for compensating for the negative effects which accompany optical radiation propagation through a randomly inhomogeneous medium by means of active control of the phase or amplitude-phase profile of optical fields in the receiving and/or transmitting channels of a system. Simultaneous real-time execution of measurements, correction, and control of the radiation wavefront is a characteristic feature of AO systems.

The active development of adaptive optics was connected with the problem of compensating for wave-

front distortions induced by atmospheric turbulence and restricting the resolution of ground-based telescopes. Then, the problem of designing high-power laser systems arose; AO systems began to be used in industry and medicine [3]. In 1989, Dreher and his colleagues created the first scanning laser ophthalmoscope with a deformable mirror [4].

Current challenges of atmospheric AO include the achievement of the diffraction quality of images formed by astronomical telescopes, ground-based aerospace object tracking, laser radiation focusing through the atmosphere, and optical communication. The importance of AO increases with the sizes of new astronomical telescopes, the energy capabilities of new laser systems, and the scope of their practical applications.

Each AO system is individually designed. The requirements for the main components and a system as a whole are determined by the atmospheric conditions of its location, in particular, by the intensity and distribution of turbulent inhomogeneities of the air refractive index over a radiation propagation path, which are characterized by seasonal, daily, hourly, and even minute variations. Therefore, the stage of designing an AO system is preceded by the stage of atmospheric measurements. It was supposed earlier [5] that atmospheric measurements were necessary only during the design stage of an AO system, and then the system could operate with incomplete information. However, it became clear later on that data on atmospheric conditions are important for the efficient

operation of AO systems. Not only real-time monitoring of atmospheric parameters is required, but also their forecast for flexible planning of scientific programs and maintenance works and selection of the instrument types with and without AO for use at a certain time.

AO systems work the best under minimal atmospheric distortions; therefore, the search for sites with minimal fluctuations of the air refractive index remains an important task in atmospheric research.

In view of the above, measuring instruments and techniques for forecasting atmospheric conditions are currently being actively developed.

1. ATMOSPHERIC ADAPTIVE OPTICS

A typical AO system for atmospheric applications includes: a radiation source, an atmospheric channel with distortions, a wavefront corrector (adaptive mirror), a wavefront sensor (WFS), and a data processing device, where measurement results are used to calculate the control signals of the wavefront corrector. The presence of additional components (WFS and wavefront corrector) is a specific feature of AO systems as electrooptical systems. The positions of the main components may differ and depends on the purpose of a system.

The efficiency of an AO system depends on several factors: principles of operation of the WFS and wavefront corrector; wavefront retrieval algorithm; correction technique; static and dynamic characteristics of the wavefront corrector and its energy parameters; corrector control algorithm; dynamic range and sensitivity of the WFS; and potential capabilities of hardware—software implementation.

The principles of operation of AO systems for atmospheric applications are based on the properties of linearity, reciprocity, and quasi-stationarity of the atmosphere [5]. Among them, the Helmholtz reciprocity principle, which corresponds to the reversibility principle, is the main one. It is performed for both free space and a turbulent medium and allows complete elimination of the effect of this medium. For the efficient operation of an atmospheric AO system, it is necessary to ensure a speed sufficient for the fulfillment of the quasi-stationarity condition, i.e., the time response of the system and the signal propagation time should not exceed the time when the turbulent medium is frozen. The problem of achieving the required performance of AO systems is still unsolved.

Let us briefly recall the stages of development of AO for astronomical applications. The first AO systems of ground-based astronomical telescopes included one WFS and one wavefront corrector and used a natural star as a reference light source. The main problem of such systems is the frequent absence of a sufficiently bright star (reference) in the isoplanar region with an astronomical object under study. To overcome that

obstacle, telescopes began to be equipped with systems for the creation of an artificial reference source — a laser guide star (LGS). The main limitation of such systems is the impossibility of compensating for the radiation wavefront slopes based on an LGS signal. As a result, the first-generation AO systems had two loops for correcting high wavefront aberrations based on an LGS signal and a loop for correcting wavefront global tilt with a natural star as guide (the requirements for isoplanatism were significantly weaker in the latter case). To develop such systems, it was sufficient to know the Fried parameter, i.e., the altitude-integral magnitude of optical turbulence of the atmosphere, but not its profile. The main disadvantages of the first-generation AO systems were the focal anisoplanatism and the limited field-of-view of the systems.

Therefore, the next state-of-the-art AO systems are multiconjugate systems which include several WFSs and wavefront correctors and use several LGSs. In these systems, adaptive mirrors are optically conjugated with different atmospheric altitudes of the strongest turbulent layers or with one altitude in the surface air layer, where the turbulence is the strongest. In the latter case, it is possible to increase the field-of-view of a system. Such systems are called ground layer AO (GL AO). For the creation and operation of such systems, detailed knowledge of the vertical distribution of atmospheric optical turbulence is required.

All AO systems for atmospheric applications can be divided into two types: active and passive. The first type includes AO systems operating along horizontal paths, first of all, systems for laser complexes. During their operation, the receiving and the emitting points are accessible; therefore, measurements along horizontal paths do not cause any particular difficulties, and if the path is considered homogeneous, interpolation of point atmospheric measurements is possible.

The second type includes AO systems operating along vertical paths: AO systems for astronomical telescopes or aerospace tracking systems, which determine the motion parameters of a self-luminous object. In this review, we mainly consider systems of the second type.

The requirements for AO system components and a system as a whole are determined by the atmospheric conditions at the system site. AO systems work best under good seeing conditions; they can fail to operate under certain atmospheric conditions. Requirements for AO are weaker in the IR region. Therefore, AO systems are individually designed, and despite apparent simplicity of the principle of operation of such systems for atmospheric problems, their elaboration is quite difficult because of many details and fine points which should be taken into account. Hence, AO systems are still quite complex and exclusive in each specific case; unique systems, e.g., for large astronomical telescopes are created by international teams.

The problem of creation of next-generation AO systems is topical today. In view of this, techniques are being actively developed for profiling atmospheric optical turbulence with the aim of determining the strongest turbulent layers and optimizing the altitudes of coupling in the atmosphere. Altitude profiles of optical turbulence parameters can differ depending on geographic coordinates, relief type, and season; they vary strongly during the day.

2. ATMOSPHERIC PARAMETERS FOR AO SYSTEMS

The main parameter which characterizes the atmospheric optical turbulence strength and the effect of atmospheric turbulence on all statistical characteristics of propagating optical radiation is the structure constant of the air refractive index C_n^2 .

The term “optical turbulence of the atmosphere,” which is in the literature on AO, is understood as the optical properties of a turbulent atmosphere. Physically, the propagation of electromagnetic waves is determined by the propagation medium, the optical properties of which are characterized by its refractive index. Turbulence in the Earth’s atmosphere produces turbulent inhomogeneities (fluctuations) of the refractive index, which cause phase and amplitude fluctuations of optical radiation propagating through the atmosphere. AO systems are to compensate for these fluctuations.

According to the Kolmogorov–Obukhov hypotheses, the structure function of the air refractive index [6] can be written in the inertial interval as

$$D_n(\mathbf{p}) = C_n^2 \mathbf{p}^{2/3}, \quad (1)$$

where \mathbf{p} is the distance between points where the refractive index is estimated. The inertial interval from the side of high spatial frequencies is bounded by the inner turbulence scale; and from the low-frequency side, by the outer turbulence scale.

The common characteristic of wavefront distortions in AO is the Fried parameter, or the coherence length of a plane wave, which determines the integral value of the atmospheric optical turbulence. This parameter is used when designing AO system components [7]. For a vertical atmospheric path, the coherence length of a plane wave

$$r_0^{\text{pl}} = \left(0.423k^2 \int_h^\infty d\xi C_n^2(\xi) \right)^{-3/5}, \quad (2)$$

where $C_n^2(\xi)$ is the altitude dependence of the structure constant of the refractive index; $k = 2\pi/\lambda$ is the wave-number, λ is the wavelength; h is the system altitude, m; x is the altitude where an artificial reference source is created.

The ratio of the telescope aperture diameter to the Fried parameter D/r_0 is a key parameter when consid-

ering the atmospheric effect on the telescope image quality. The telescope size is classified in terms of this parameter: middle-size telescopes ($D/r_0 = 10$), small telescopes ($D/r_0 < 10$), and large telescopes ($D/r_0 > 10$).

The isoplanatism zone is calculated in AO through the isoplanatic angle

$$\theta_0 = \left(2.91k^2 (\sec \vartheta)^{8/3} \int_0^\infty d\xi \xi^{5/3} C_n^2(\xi) \right)^{-3/5}, \quad (3)$$

which determines the region in the atmosphere where the wavefronts of radiation from a reference object and an object under study are equally phase distorted while propagating.

The altitude profile of optical turbulence along with the wind speed profile determines the requirements for the speed of the AO system of a ground-based telescope via the Greenwood frequency, or the atmospheric coherence time

$$\tau_0 = \left(2.91k^2 \sec \vartheta \int_0^\infty d\xi C_n^2(\xi) V_{\text{wind}}^{5/3}(\xi) \right)^{-3/5}, \quad (4)$$

where ϑ is the zenith angle, and $V_{\text{wind}}(\xi)$ is the altitude profile of the wind speed.

The wind determines the time frequency of wavefront fluctuations and affects the optical turbulence strength, since the wind speed gradient induces atmospheric turbulence generation. Surface wind produces vibrations of a telescope, and, hence, jitters of images formed by the telescope. The AO system speed linearly increases with the wind speed. Therefore, wind speed is an atmospheric parameter, the knowledge of which is also important for AO systems. Techniques for measuring the wind speed are well known in meteorology. As for the AO systems, we deal not with the wind speed, but with the time scales of wavefront fluctuations. Therefore, almost all the optical techniques for determining $C_n^2(\xi)$ described below make it possible to estimate the speed of motion of turbulent layers.

Thus, to solve AO problems, one should know the following parameters defined via the structure constant of the air refractive index: the Fried parameter r_0

or the profile $C_n^2(\xi)$, the isoplanatic angle θ_0 , and the coherence time τ_0 or the wind speed V_{wind} . These parameters determine the spatiotemporal characteristics of an AO system and requirements for the design of system components—wavefront sensors and correctors (the number of components, the focal length of the microlens array, the number of control channels of an adaptive mirror, etc.).

3. TECHNIQUES AND INSTRUMENTS FOR MEASURING ATMOSPHERIC OPTICAL TURBULENCE

Techniques for estimating $C_n^2(\xi)$ can be divided into *optical* and *acoustic* according to the physical principle underlying the measurements. Another classification principle, in terms of the measurement region, was introduced in [8]: measurements in the surface air layer and in the free atmosphere. The turbulence of the lower atmosphere makes the greatest contribution (from 40 to 80%) to the degradation of optical images made by a ground-based telescope.

3.1. Optical Techniques

Optical techniques can be grouped by the physical principle underlying them: measurements of phase fluctuations and measurements of radiation intensity fluctuations.

Note that our review is not exhaustive, because AO methods are currently being actively developed. Many approaches to measurements of atmospheric optical turbulence and wind speed have been suggested. However, they are just modifications of the optical techniques we consider, which have already shown their effectiveness in long-term atmospheric measurements.

Stock and Keller suggested [9] the concept of a differential technique for estimating the image quality in the 1960s. The technique consisted in measurement of the variance of random shifts of the energy center of gravity of two images of the same star made by different parts of the lens. The main advantage of the technique is the possibility of distinguishing between mechanical vibrations of the instrument and the measured jitters due to atmospheric turbulence.

That concept was implemented by researchers from the European Southern Observatory [10] when coordinate-sensitive receivers were created. In that work, a CCD array was used for objective estimation of shifts of two star images relative to each other. The instrument created was called DIMM (Differential Image Motion Monitor).

The variance of the difference signal is connected the coherence length of an optical wave (r_0), which characterizes the turbulence integral over the radiation propagation path:

$$\sigma_{1,t}^2 = K_{1,t} \lambda^2 D_{\text{sub}}^{-1/3} r_0^{-5/3}, \quad (5)$$

$$\sigma_{\phi}^2 = \frac{1}{2}(\sigma_1^2 + \sigma_t^2), \quad (6)$$

where $\sigma_{1,t}^2$ is the variance of radiation fluctuations in the longitudinal and transverse directions; D_{sub} is the subaperture diameter; $K_{1,t}$ are the coefficients of wavefront slope type measured as functions of the subaperture size and the distance between them. Equa-

tions for the coefficients as functions of the slope measured (G - and Z -slopes) are given in [11].

For the practical implementation of this method, a mask with two subapertures is fixed at the receiving aperture of a small telescope (25–50 cm), and the radiation is usually split with an optical wedge. The σ^2 calculation accuracy depends on the accuracy of determining the instantaneous coordinates of each of the two shifting images and, therefore, affects the r_0 estimation accuracy. The instrument noise results in the errors in coordinates. The pixel size, the camera exposure time, and the number of frames are important parameters; their effects were studied in [12].

Let us describe features of DIMMs for astronomical applications. The point spread function (PSF) width at half maximum (FWHM), also called seeing (ε_0), is usually used for estimation of the image quality in astronomical observations. In a DIMM, ε_0 is usually approximately estimated at $\lambda = 0.5 \mu\text{m}$ as

$$\varepsilon_0 \approx 0.98 \frac{\lambda}{r_0}. \quad (7)$$

Note that a DIMM measures r_0 , which characterizes atmospheric conditions, i.e., the seeing of an observatory, instead of the PSF of a telescope, and then ε_0 is calculated by the DIMM software. Therefore, seeing is not the image quality here, but a characteristic of the atmosphere, while the PSF characterizes an image, but not the atmosphere or seeing conditions. The atmosphere is the main, but not the only, contributor to the deterioration of the telescope image quality. The shape and width of the PSF of a telescope operating through the Earth's atmosphere are determined by instrumental PSF and the PSF due to atmospheric and dome turbulence (dome seeing).

A device similar to DIMM was created at the IAO SB RAS in 1998. It was based on the same physical principles but used laser radiation along horizontal atmospheric paths. It was called a differential turbulence meter (DTM) [13] (Fig. 1).

A Maksutov-type mirror–lens telescope AZT-7 was used in the first DTM version, and then DTM was modernized: a TAL telescope with an aperture of 0.2 m and four subapertures was used [14]; C_n^2 was estimated accounting the formula for the laser beam coherence length:

$$C_n^2 = \frac{\sigma_{1,t}^2}{1.411 \pi^2 L (0.157 D_{\text{sub}}^{-1/3} - 0.145 d^{-1/3})}, \quad (8)$$

(d is the distance between the subapertures).

A device for daytime image jitter measurements on the basis of differential technique was called SDIMM. The Sun was used as a radiation source; modifications consisted in the use of appropriate filters [15].

Kornilov and Tokovin improved the DIMM by adding a turbulence profiler, which was based on the

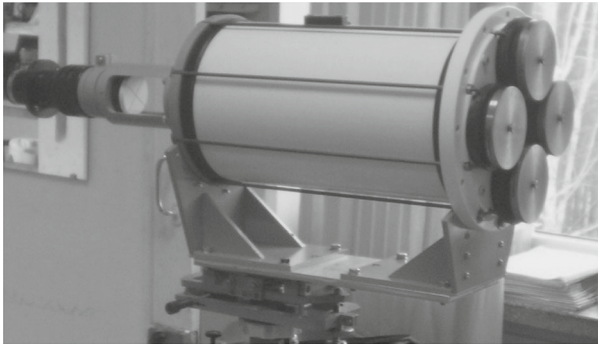


Fig. 1. Differential turbulence meter.

statistical analysis of star scintillations measured at four ring apertures of MASS (Multi Aperture Scintillation Sensor) [16]. The idea of using radiation intensity fluctuations for measurement of atmospheric optical turbulence was suggested by Clifford [17]. The technique was developed for astronomical application in works by Tokovin [18].

The differential image scintillation index in the region of weak fluctuations

$$\sigma_I^2 = \int W(h)C_n^2(h)dh, \quad (9)$$

where $W_x(h)$ are the weight functions dependent on the radiation propagation geometry (receiving aperture size, angular size of a radiating object, and radiation wavelength).

The smallest aperture (2 cm diameter) in MASS is sensitive to turbulence at low altitudes, on the order of 0.5 km, and the largest aperture (13 cm outer diameter) is mainly sensitive to turbulence in high atmospheric layers. The statistical analysis of scintillations (radiation amplitude fluctuations) in all the four apertures makes it possible to distinguish between turbulent layers and to measure the turbulence strength in each of them, and then, inverting Eq. (17), to retrieve C_n^2 of individual layers. This method provides a low resolution and is insensitive to the near-surface turbulent layer, but it is simple and robust. Instrumental and other factors of the measurement accuracy are considered in [19].

Note that almost all existing astronomical observatories use DIMMs at different commercial small telescopes, mainly of the Cassegrain scheme. MASS-DIMMs were actively used for selection of sites for new telescopes and are now used at telescope sites to support the operation of AO systems.

Two triangulation techniques are commonly used for $C_n^2(\xi)$ vertical profiling: SLODAR and SCIDAR, where the atmospheric optical turbulence profile is retrieved from the correlation between wavefront slopes (SLODAR) or scintillation intensity patterns

(SCIDAR) of two stars with a known angular distance between them.

The SCIDAR (SCIntillation Detection and Ranging) technique was suggested by Vernin and Roddier in 1973. It is based on the analysis of the cross-correlations of scintillations of each star in a binary star. The technique allows retrieving not only the turbulence profile $C_n^2(\xi)$, but also the velocity of the turbulent layer $V(\xi)$ as a function of altitude from short-exposure images of binary star scintillations [20]. In the approximation of weak fluctuations, the 3D power spectrum of fluctuations in the air refractive index and the 2D spectrum of radiation scintillations in the observation plane are related. The radiation from two stars separated by the angle θ passes through a turbulent layer at an altitude H , the scintillation of one star at the receiver is shifted relative to another to the distance $H\theta$. The spatial autocovariance of the scintillations has a peak at $r = \pm\theta H$, which is proportional to C_n^2 of this layer:

$$C(r - \theta H) = \int dh C_n^2(h) \delta H K(r - \theta H), \quad (10)$$

where δH is the altitude resolution; $K(r - \theta H)$ is the theoretical covariance function of scintillations. $C_n^2(\xi)$ can be retrieved from measurements of the covariance function of the scintillations in the telescope pupil and calculations of $K(r - \theta H)$.

The technique is limited because it is insensitive to the turbulence of the surface layer h_0 , since its contribution is proportional to 5/6 at each altitude. The limitation can be overcome by shifting the measurement plane below the telescope pupil plane.

The theoretical resolution of SCIDAR is determined by the size of the Fresnel zone for a turbulent layer altitude specified. We emphasize that SCIDAR and its modifications require a large (at least 2 m) telescope to ensure a high resolution in the surface air layer [21]. In addition, it is often difficult to find binary stars with a large angular separation, especially with the required stellar brightness.

The modified stereo-SCIDAR approach uses a stereoscopic system, where scintillations of each binary star are detected by a separate detector [22]. In the previous implementations of SCIDAR, the scintillations of two stars were usually superimposed on each other in one detector. Separation of star images has several advantages. Visualization of scintillations of each individual star increases a possible difference in the stellar magnitudes, which increases the number of available sources the instrument can use. In addition, as compared to a single SCIDAR camera, the signal-to-noise ratio of a turbulence profile retrieved increases with the difference in magnitude between the stars in a pair: by a factor of two for stars of the same magnitude and by a factor of 6.3 for stars different in brightness by two magnitudes. If two stars differ

in brightness by 2.7 magnitudes, then the sensitivity of stereo-SCIDAR increases by a factor of 12 as compared to SCIDAR with a single camera. The methods are implemented in devices mounted in the largest Mauna Kea and Paranal Astronomical Observatories [21, 22].

In the SLODAR (SLOpe Detection And Ranging) method, the altitude profile of the turbulence is retrieved from the time average spatial-angular cross-correlation function of local wavefront slopes measured in the telescope lens plane with a Shack–Hartmann WFS on the basis of observations of a binary star [23].

The complete normalized profile of $C_n^2(h)$ is retrieved from the cross-correlation function via deconvolution, where the cross-correlation of the wavefront slopes for each of the stars of a binary star is used as a measure of the system's pulsed response to a single turbulent layer.

A turbulent profile is estimated from Shack–Hartmann sensor data as follows. Short-exposure hartmannograms are simultaneously recorded for each star. The wavefront slopes are calculated for each subaperture of the sensor on two spots for each of the orthogonal directions i and j . The slope averaged over all illuminated subapertures is subtracted from the individual slopes for each star; this eliminates the influence of the telescope pointing error common to all subapertures. If $s_{i,j}$ is the slope of the radiation wavefront from the 1st star on the subaperture (i, j) at time t and $s'_{i,j}$ is the wavefront slope of the radiation from the 2nd star on the corresponding subaperture, then the spatial cross-correlation function of the measured slopes

$$C(\delta_i, \delta_j) = \left\langle \sum_{i,j} s_{i,j}(t) s'_{i+\delta_i, j+\delta_j}(t) / O(\delta_i, \delta_j) \right\rangle. \quad (11)$$

Here, the angle brackets mean the averaging over all independent WFS frames; $O(\delta_i, \delta_j)$ is the number of overlapping subapertures (with available data on slopes) for the shift (δ_i, δ_j) .

The cross-correlation for an individual star is estimated in the same way:

$$A(\delta_i, \delta_j) = \left\langle \sum_{i,j} s_{i,j}(t) s_{i+\delta_i, j+\delta_j}(t) / O(\delta_i, \delta_j) \right\rangle. \quad (12)$$

$A(\delta_i, \delta_j)$ is the assessment of the effect of a single turbulent layer, which is used for the optical turbulence profiling via deconvolution. The normalized $C_n^2(h)$ profile is retrieved with the use of the one-dimensional Fourier transform:

$$C_n^2 \propto F^{-1}[F[C]/F[A]]. \quad (13)$$

The advantage of the method is its sensitivity to turbulence at all altitudes, including ground level, with a response function which weakly depends on the alti-

tude. The wind speed in an individual turbulent layer can be determined from the cross-correlation function of the wavefront slopes calculated with a nonzero delay between imaging the centroids of two stars at the WFS. In this case, each peak in the two-dimensional cross-correlation functions is shifted relative to its position for zero delay by an amount proportional to the corresponding wind speed in the layer.

The vertical resolution δH of the method is related to the binary star separation angle θ as

$$\delta H = \frac{D/n_{\text{sub}}}{\theta}, \quad (14)$$

where n_{sub} is the number of subapertures in the projection on the telescope pupil w .

The maximal altitude

$$H_{\text{max}} = n_{\text{sub}} \delta H. \quad (15)$$

The larger the telescope aperture diameter, the higher the sensing altitude. When using a telescope with an aperture 0.4 m in size, the maximum altitude is ~ 1 km, the resolution is 1 arcsec. Therefore, to attain acceptable performance, the method should be used for large telescopes.

The method modification SL (surface layer)-SLODAR for supporting GLAO systems is limited to a sensing altitude of 500 m, but provides for an altitude resolution of 10 m when working with a small telescope with an aperture of ~ 0.5 m [24].

It is often difficult to use double stars with a large angular separation, especially with a reasonable difference between stellar magnitudes. To overcome this obstacle, a device has been developed and is now operated at the Kalern Observatory and at the South African Astronomical Observatory. It allows reconstructing $C_n^2(h)$ from observations of the moon limb and the solar limb in night and day hours. Parts of the moon limb are considered as a double star. The spatial and temporal cross-correlation functions of the wavefront arrival angles are used to profile optical turbulence and associated parameters [25, 26].

Let us note a possibility of using a Shack–Hartmann sensor in an AO system loop for measuring optical turbulence, i.e., for turbulence profiling by the SLODAR method and for retrieving r_0 (13) by the differential method from image jitter measurements at two sensor subapertures. Such measurements of the Fried parameter have been implemented at large solar telescopes, including the Large Solar Vacuum Telescope (LSVT) of the Baikal Astrophysical Observatory, where a Shack–Hartmann WFS is used as a differential turbulence meter in the AO system correction loop [27, 28]. A Shack–Hartmann WFS in AO systems of solar telescopes measures Z-slopes. A WFS is used to profile $C_n^2(\xi)$ in the AO system of the solar telescope of the Big Bear Observatory, United States [29]. Four WFSs operate in the AO system of the Very Large

Table 1. Optical instruments for measuring atmospheric optical turbulence

Instrument	$C_n^2(h)$	Telescope aperture diameter	Note	Technique
DIMM	r_0	20–50 cm; small commercial telescope and mounting	Telescope modification is required	Phase fluctuations
SLODAR	+	1–2 m	Double star is required	Phase fluctuations
MASS	+	25–50 cm; commercial telescope and mounting	Low resolution; does not measure surface turbulence	Intensity fluctuations
SCIDAR	+	2 m	Double star is required	Intensity fluctuations
Shack–Hartman WFS	+, r_0	Any	In the AO system loop	Phase fluctuations
Turbulent lidar	+	Small telescope	Horizontal path	Intensity fluctuations

Telescope (VLT) by signals from four LGSs [30]; they are also used for optical turbulence profiling. AO systems provide for results directly at the telescope point at a required time, which is important for the efficient operation of the telescope AO systems.

Lidars play an important role in atmospheric research. They have a number of advantages, including high temporal resolution and wide spatial vertical coverage. Lidar methods for wind speed profiling have been actively developed since the 1980s, including at the IAO SB RAS. Several approaches were suggested and developed for diagnosing and studying the boundary air layer using lidars [31].

The use of lidars for C_n^2 estimation is also promising [32]. Such a method is being actively developed by Razenkov at the IAO SB RAS (e.g., [33]) based on the effect of backscatter enhancement of the average echo power using Vorob'ev's approximation for the C_n^2 profile [34]:

$$\tilde{C}_n^2(x) = \frac{q(x, R, C_n^2) \left[1 + 0.4R^2 / r_F^2(x) \right]^{7/6}}{0.49k^{7/6} x^{11/6}}, \quad (16)$$

where \tilde{C}_n^2 is the lidar estimate of the structure constant of the air refractive index; $r_F(x) = \sqrt{x/k_0}$ is the Fresnel scale, x is the distance to the lidar; q is the factor of the turbulence effect on the average power of scattered radiation at the receiver; R is the radius of the receiving lidar aperture.

This technique apparently allows detecting large-scale vortex and wave structures and, therefore, can become an alternative to sodars. The technique is limited by lidar operation at weakly inclined sensing paths with respect to the horizon. Lidars were previously suggested to be used for atmospheric turbulence sensing, but that time the lidar technique was a combination of the DIMM differential method with LGS [35].

Table 1 summarizes the features of the techniques for atmospheric optical turbulence measurements considered in this section. Let us briefly compare them.

SLODAR and SCIDAR require a telescope with an aperture size of at least 1.5 m. Therefore, instruments based on them cannot be used as mobile equipment for atmospheric measurements, but allow $C_n^2(\xi)$ profiling, which is necessary for contemporary AO systems.

DIMMs require a telescope modification, but, like MASS, are assembled from commercially available equipment (mounting, small telescope, etc.); therefore, they are easily transportable. In addition, they can be mounted in a small dome (diameter <3 m) and their operation can be fully automated. Scintillation meters are often insensitive to surface turbulence (0.5 km). A Shack–Hartmann WFS in the AO system loop does not require an additional telescope; measurements are carried out directly at the telescope point, which is especially important for the efficient operation of an AO system.

3.2. Acoustic Techniques

The review would be incomplete without consideration of acoustic measuring instruments: sodars and ultrasonic thermoanemometers. In acoustic sounding, sound waves propagating in the atmosphere are scattered by wind and air temperature field inhomogeneities, which are primarily associated with turbulent motion.

Sodar is a remote sounding system which provides information on the turbulence strength, temperature, and wind gradients from measurements of the sound backscatter intensity profile. The distance to scatterers is determined by the delay of a signal reflected; the turbulence strength can be estimated by the reflected signal power, and the wind projection on the sounding direction is determined by the Doppler frequency shift. The advantage of sodars is their relative simplicity, reasonable price, and reliability of measurements at a quite high vertical resolution (on the order of 5–50 m). The main disadvantages of sodars are the limited vertical detection range (from a few hundred meters to 1 km) and low data availability under certain weather conditions. In addition, a signal emitted (usually 1–10 kHz) is audible to man.

A series of acoustic systems for atmospheric sounding (sodars) were developed at the IAO SB RAS: “Zvuk-1,” “Zvuk-2,” “Volna-3,” and “Volna-4.” They are mobile towed complexes consisting of one or three acoustic antennas and a control cabin [36]. These systems measure vertical profiles of wind speed, temperature, and the turbulence parameter in the altitude range from 40 to 1000 m.

The acoustic sounding technique was used for monitoring an optically active turbulence in the atmospheric boundary layer already in the late 1980s. [37]. Combined experiments were carried out at several mountain astronomical observatories of the former Soviet Union to explain the difference in the quality of astronomical images at different sites. In [38], optical measurements were accompanied by turbulence observations with a high-resolution sodar specially designed for this purpose at the Concordia Astronomical Observatory (Antarctica). Sodars were used to search for a site for the TMT telescope [39].

The simplest acoustic device is an ultrasonic thermoanemometer, which measures the structure constant of the temperature and certain turbulent parameters in the surface air layer. Portable thermoanemometers, ultrasonic meteorological stations “Meteo-2” created at the IAO SB RAS, and the acoustic meteorological complex (AMC) of the Institute of Monitoring of Climatic and Ecological Systems, Siberian Branch, Russian Academy of Sciences, allow estimating the structure function of the air refractive index [40]:

$$C_n^2(h) = C_T^2(h) \left[\frac{80 \times 10^{-6} P(h)}{T(h)} \right]^2, \quad (17)$$

where C_T^2 is the structure constant of the temperature T ; P is the pressure.

These inexpensive mobile devices can be fixed on a weather mast and used in cold climate areas [41]. Their main disadvantage is point measurements, which, however, can be approximated for homogeneous paths. An alternative is to use several ultrasonic thermoanemometers.

Comparative measurements with an acoustic weather station and by optical methods (DIT, Shack–Hartmann WFS) were performed in [42, 43]. The results show a high correlation, but differ in absolute values. In general, thermoanemometer measurements for AO are useful both for laser systems operating along horizontal paths and for studying the physics of atmospheric turbulence generation in the boundary layer above observatory sites.

4. MODERN PROBLEMS IN ATMOSPHERIC RESEARCH FOR AO

Today, almost all large telescopes are equipped with AO systems, including multistage systems, which are being continuously improved [44–49]. When creating

new telescopes, AO systems are already being developed in the design stage [50, 51].

Worldwide observatories have accumulated volumes of statistical information on optical turbulence [52, 53].

This allows developing models of not only the C_n^2 altitude profile, but also the wind speed profile based on the Bufton model [54]. Atmospheric measurements are performed in the monitoring mode, often simultaneously by several methods. For example, a recent study [55] compares data from stereo-SLODAR, MASS-DIMM, and Shack–Hartmann WFS of the VLT AO system at the Paranal Observatory. The data are consistent, which indicates the effectiveness of all methods used and the reliability of the results.

The forecast of atmospheric conditions, including optical turbulence and other seeing parameters, is an urgent task of atmospheric research for AO. It is of fundamental importance for all types of AO systems, for flexible scheduling of astronomical observations, and efficient operation of telescopes. This is confirmed by the program for the search for a reliable technique for predicting atmospheric optical turbulence and meteorological conditions, which was announced in 2020 by the European Southern Observatory – the largest astronomical association. A request [49] was published to find institutions capable of developing a system for predicting turbulence and meteorological conditions (for three nights, and, with higher accuracy, for the night to come) at the Paranal Observatory [56, 57].

There are several types of forecasts of atmospheric conditions in astronomical observatories: for 14 h; for short intervals of 1–4 h; for 15–20 min, which are of interest for the efficient operation of AO systems [58]; the search for time intervals with a high isoplanatic angle and coherence time from 20 min to 2 h for a quick choice of instrument (for example, the spectrograph type); and of attainable quality of telescope images (ϵ_0), i.e., $C_n^2(\xi)$, for several days.

The problem of predicting optical turbulence and related parameters is mainly solved with the use of numerical weather forecast models. The Masciadri group is developing the Astro-Meso-Nh nonhydrostatic model for forecasting seeing parameters, including turbulent characteristics [58, 59]. The model was used in Chile.

The European Center for Medium-Range Weather Forecasts (ECMWF) model was used in [60]. The Mauna Kea Weather Center (MKWC) model [61] is applied for optical turbulence forecast at the Mauna Kea Observatory (Hawaii). The Weather Research and Forecasting (WRF) model was tested by the authors of [62] at observatories located on the Tibetan Plateau.

However, the optical turbulence forecasts are imperfect. Therefore, seasonal calibrations based on long-term ground-based measurements, e.g., with

MASS-DIMM, are used. However, even this solution does not always lead to a satisfactory forecast [59]. In [63], the authors additionally use autoregressive models, which improve forecasts under good seeing conditions and for short periods of time, since the technique is actually a forecast by the last value. The authors of the above studies suggest using other mathematical methods for time series prediction, such as the Kalman filter along with Astro-Meso-Nh.

The task of forecasting atmospheric conditions is related to the accuracy of the parameterization of an optical turbulence in the lower atmosphere. Therefore, a possible solution is to use a weather forecast model along with the surface air layer model based on the Monin–Obukhov similarity theory [64]. The properties and dynamics of the layer are largely determined by its interaction with the underlying surface, which can be characterized by turbulent fluxes of momentum, heat, and moisture. The Monin–Obukhov similarity theory predicts well turbulence physics under unstable and neutral atmospheric stratification, but is inapplicable in the case of stable stratification; i.e., it can be used for a flat homogeneous underlying surface under the assumption of stationarity and homogeneity of meteorological fields. The spectrum of fluctuations of the refractive index of air in the inertial range of wavenumbers obeys the $-5/3$ power law, which often does not meet to the conditions of mountain observatories. Therefore, the theory should be modified for them or it is necessary to apply entirely different approaches. The study of the optical characteristics of a turbulent atmosphere under these conditions is a separate task.

Other modern approaches to forecasting C_n^2 in the lower atmosphere include machine learning methods, which have become popular in various fields in recent years. In 2016, it was first suggested to use an artificial neural network (ANN), which was a multilayer perceptron, to estimate C_n^2 through air temperature, pressure, and relative humidity at the Mauna Loa observatory [65]. The correlation coefficient was calculated to be high (0.8) between the values measured and the ANN estimates for neutral and unstable atmospheric stratification, where the Monin–Obukhov theory is applicable, and equal to 0.6 for a stably stratified atmosphere. It is necessary to know the functional relationships between the parameters and to select the weights of the connections in the learning process for this ANN to work, which makes it difficult to use the ANN with other data. The ANN is a black box model.

In [66], the “random forest” machine learning method is used to forecast the structure constant of the surface air refractive index near the sea and to study the contribution of meteorological parameters to optical turbulence generation. However, the authors do not mention the atmospheric stratification type and statistical errors; they only point to the usefulness of the method.

In [67], a backpropagation neural network optimized by an adaptive genetic algorithm was successfully applied for forecasting meteorological parameters; a correlation coefficient was equal to 0.93 under Antarctic conditions, i.e., under weak atmospheric optical turbulence.

All the above forecasts using machine learning methods are based on ultrasonic thermoanemometer measurements of atmospheric air characteristics.

5. ATMOSPHERIC RESEARCH AT RUSSIAN ASTRONOMICAL OBSERVATORIES

The Large Solar Vacuum Telescope of the Baikal Astrophysical Observatory (BAO) of ISTP SB RAS is the only Russian telescope equipped with an AO system today [68–70]. The system was developed at the IAO SB RAS.

The study of the seeing conditions in the world began within the search for best sites for astronomical telescopes with minimal atmospheric optical disturbances. Note the equivalence of the terms “optical state of the atmosphere” (common in the atmospheric optics) and “seeing conditions” understood as a set of atmospheric conditions which affect optical radiation propagating through the atmosphere. The quality of astronomical observations is affected not only by turbulence, but also by other factors (cloudiness, aerosol, etc.) of the optical state of the atmosphere.

Studies of seeing conditions were actively developed in the Soviet Union until the 1990s; numerous acoustic and optical measurements were carried out [37, 71]. Generalization of the results of seeing condition studies, including turbulent characteristics, can be found in [72, 73]. Then, judging by the lack of publications, those works were almost stopped in the main Russian observatories.

At that time, atmospheric (seeing) research for AO was continued in foreign observatories where large telescopes were located or were planned to be mounted. The main attention was paid to the parameters associated with atmospheric optical turbulence and wind speed. During that period, a new parameter, that is, the wind speed at a level of 200 hPa (V200), was introduced to estimate the applicability of AO systems. The correlation between that parameter and the astronomical image quality was ascertained for a number of large astronomical observatories [74–79], including the BAO [80]. This parameter is connected with the AO system frequency as $\bar{V} = bV200$ (b is a coefficient). Vertical gradients in V200 induce a clear-sky turbulence.

One of the approaches to the study of seeing conditions is the use of a meteorological reanalysis. It was applied to the study of the altitude distribution of wind speed in all large astronomical observatories [72–80]. A meteorological reanalysis includes different atmospheric measurements; radiosonde, aircraft, and sat-

ellite observations, and other data and is a result of assimilation of these data at the nodes of a regular grid over the Earth. The use of reanalysis data and satellite measurements can be useful for studying current and long-term variations in other seeing parameters, such as cloudiness and precipitable water vapor [81, 82].

Figure 2 shows the distribution of wind speed at a level of 200 hPa for two regions, southern Siberia and the North Caucasus, according to reanalysis data [83, 84]. From the point of view of the frequency characteristics of an AO system, the BAO is in better conditions than the Sayan Solar Observatory (SSO). The question of the best place for the Large Altazimuth Telescope (BTA) in Russia is still debatable. There are no points with low V200 in the Caucasus Mountains. The Crimean Astrophysical Observatory is the best in terms of this parameter.

Figure 3 shows histograms of V200 distribution in 1948–2018 from the NCEP/NCAR reanalysis data for BAO and SSO. They witness different atmospheric conditions in the Russian astronomical observatories.

As is ascertained in [80] on the basis of coherence length measurements, the higher V200 at the BAO, the worse the astronomical quality of daytime images (the higher the daytime ϵ_0). There are no experimental data on the dependence between these parameters for the BTA site. Assuming such a relationship, the best time for the BTA AO system operation is from October to May, in contrast to the BAO, where the best time for astronomical observations is from June to September. According to [81], V200 has been changing due to climate change in recent years, decreasing or increasing in different observatories.

As already mentioned in Section 4, modern seeing research is aimed at forecasting atmospheric conditions, including for the efficient operation of AO systems. In foreign observatories, atmospheric parameters are often monitored simultaneously with several instruments; statistical data have been accumulated. In the Russian Federation, there is an astronomical seeing post at the Caucasian Mountain Observatory (CMO) of the Sternberg Astronomical Institute of Moscow State University, where all parameters necessary for the AO system design have been monitored with MASS-DIMM since 2007 [85, 86]. As a result, seasonal features of the isoplanatism and coherence time are known (median $\tau = 6.57$ ms). DIMM measurements are carried out by the ISTEP SB RAS at the SSO [87]. Study of the atmospheric conditions of the BAO ISTEP SB RAS, including the seasonal statistics of the Fried parameter measured by the correlation Shack–Hartmann WFS of the LSVT AO system, is described in [28, 80, 88]. Histograms of the distribution of the structure constant of the air refractive index measured with a Meteo-2 ultrasonic weather station in the surface air layer in different seasons are given in [89].

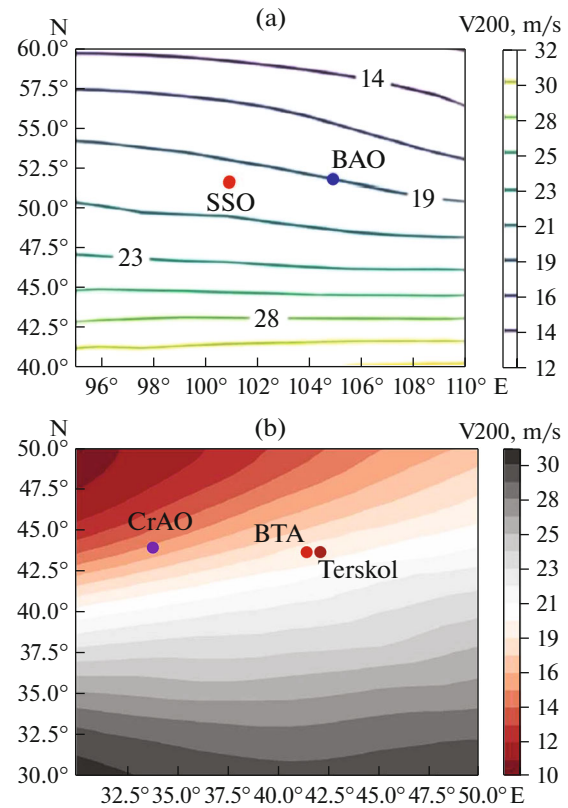


Fig. 2. Average distribution of V200 based on ERA Interim reanalysis for observatories of (a) southern Siberia [76] and (b) North Caucasus (adapted from [77]).

Several important results about the turbulent regime of the lower atmosphere at observatories in southern Siberia were derived from measurements with ultrasonic weather stations (complexes) AMK and Meteo-2 in [90–94, 96]. The first result is the detection of a coherent non-Kolmogorov turbulence which weakens the optical radiation fluctuations. In practice, this effect means the presence of time windows with high image quality. These coherent structures reduce the telescope image jitters more than two times at SSO. Similar, but not as long-term, studies were carried out at the Special Astrophysical Observatory (SAO), Russian Academy of Sciences. Generation of vortex coherent structure under certain meteorological conditions was shown in [95]. The results of the study of generation of optical turbulence in the lower atmosphere in the observatories in southern Siberia are summarized in [96, 97].

There are no measurement data on the Fried parameter (atmospheric optical turbulence profile) and other parameters required for designing AO systems for the largest Russian telescope, the BTA, over the past 10 years. Turbulent characteristics are not monitored for the Crimean Astrophysical Observatory, which is one of the largest observatories of the former Soviet Union. There are no statistical data for

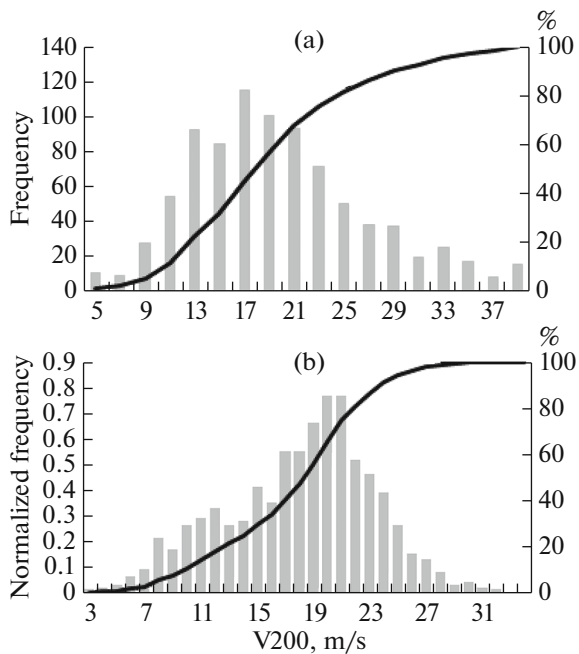


Fig. 3. Histogram of V200 from 1948 to 2018 based on NCEP/NCAR reanalysis for (a) SAO RAS [84] and (b) BAO ISTP SB RAS [80].

the Terskol Observatory in the literature, except for the measurements of the 1980s [37, 98]. In other words, Russian astronomical observatories do not monitor optical turbulence and related parameters and do not perform full-scale atmospheric studies, which does not allow equipping RF telescopes with AO systems. The only exception is the CMO MSU, where atmospheric measurements are carried out and the accumulated results make it possible to start designing an AO system.

The use of optical turbulence measurements in 1980–1990s in Russian observatories (see Table 3, [37, 98]) seems incorrect for the development of AO systems due to climate changes, which, as is shown on the example of Chile observatories [99] on the basis of reanalysis data and field measurements, have been changing the seeing conditions since 2000s.

Astronomical observations are influenced not only by optical turbulence, but also meteorological factors, such as the precipitable water vapor, aerosol, and cloudiness. In general, the seeing at a telescope site is an important factor of the quality of the telescope work. Forecasting atmospheric conditions in observatories will help to increase the efficiency of astronomical telescopes.

CONCLUSIONS

The forecast of atmospheric conditions is currently the main direction in the development of atmospheric research for AO problems. Monitoring, statistical

data, and modeling the structure constant of the air refractive index have surely not lost their relevance.

The search for sites with minimal C_n^2 remains an important task. But a possibility of forecasting time windows with high or low values of the main atmospheric parameters (coherence length and time and isoplanatism) is important for improving the efficiency of AO systems and telescopes in general.

The main trend in this direction is the use of machine learning methods. The progress achieved with the help of mathematical methods encounters a number of unsolved AO problems which limit the forecast quality, namely, possible restrictions imposed by the Earth's atmosphere on optical radiation propagation, first of all, optical turbulence in the lower atmosphere in the case of deviations from classical theories: non-Kolmogorov, coherent turbulence and stable stratification (stable atmosphere).

The development of the theory of the stably stratified surface air layer, i.e., where the gradient Richardson number is positive and the Monin–Obukhov theory is inapplicable, is the subject of many works, but this problem of atmospheric physics has not yet been solved. Optical properties of atmospheric turbulence in this case are of particular interest, since these conditions are mainly implemented in nighttime in mountainous regions, and the surface layer mainly contributes to the distortions of optical images formed by a ground-based telescope. Clear-air turbulence, which most often occurs in mountainous regions, is also of interest.

Many works are devoted to the study of optical radiation propagation when the exponent deviates from classical in the models of power density of air refractive index fluctuations under so-called non-Kolmogorov turbulence, but these studies mainly concern laser beams. Atmospheric measurements with the use of modern lidar and acoustic techniques seem to be useful for solving the above problems.

A clear trend towards profilers is observed in the development of instrumentation for next-generation AO systems. However, the DIMM remains the most common instrument for systematic atmospheric measurements, since it allows using small commercial telescopes, in contrast to profiling methods which require telescopes with apertures at least 1.5 m in size. The use of wavefront sensors in AO systems of a telescope seems promising, including for profiling the structure constant of the air refractive index.

Let us once again note a need for atmospheric measurements at Russian observatories in connection with the importance of equipping existing telescopes with AO systems for their efficient operation. Such seeing parameters as cloudiness, moisture content, and aerosol undoubtedly affect the efficiency of astronomical observations, but random inhomogeneities in the refractive index during turbulent motion in the atmosphere reduce the resolution of optical tele-

scopes. A radical solution to this problem is equipping telescopes with AO systems designed with atmospheric measurements taken into account. Understanding the atmospheric effect on imaging is the starting point for designing AO systems.

In addition, studies of seeing conditions are necessary for better understanding of possible limitations imposed by the Earth's atmosphere. This knowledge and statistics of seeing parameters support modeling, forecasting, developing a strategy of using telescopes, and planning astronomical observations. Creation of systems for forecasting atmospheric conditions, not only turbulent, is one of the ways of increasing the efficiency of astronomical observations with the existing Russian telescopes.

Note that measurements of the outer atmospheric turbulence scale and turbulence of the dome space of a telescope and the study of parameters of a layer of sodium and other metals for creation of LGS systems of telescope AO remained beyond the scope of this review.

FUNDING

The work was supported by the Russian Foundation for Basic Research (project no. 20-12-50249).

CONFLICT OF INTEREST

The authors declare that they have no conflicts of interest.

OPEN ACCESS

This article is licensed under a Creative Commons Attribution 4.0 International License, which permits use, sharing, adaptation, distribution and reproduction in any medium or format, as long as you give appropriate credit to the original author(s) and the source, provide a link to the Creative Commons license, and indicate if changes were made. The images or other third party material in this article are included in the article's Creative Commons license, unless indicated otherwise in a credit line to the material. If material is not included in the article's Creative Commons license and your intended use is not permitted by statutory regulation or exceeds the permitted use, you will need to obtain permission directly from the copyright holder. To view a copy of this license, visit <http://creativecommons.org/licenses/by/4.0/>.

REFERENCES

1. H. W. Babcock, "The possibility of compensating astronomical seeing," *Publ. Astronom. Soc. Pac.* **65** (386), 229–236 (1953).
2. V. P. Linnik, "A possibility in principle of changing the atmospheric effect on star images," *Opt. Spektrosk.* **25** (4), 401–402 (1957).
3. J. A. Kubby, *Adaptive Optics for Biological Imaging* (CRC Press, Boca Raton, FL, 2013).
4. A. W. Dreher, J. F. Bille, and R. N. Weinreb, "Active optical depth resolution improvement of the laser tomographic scanner," *Appl. Opt.* **28**, 804–808 (1989).
5. V. P. Lukin, *Atmospheric Adaptive Optics* (Nauka, Novosibirsk, 1986) [in Russian].
6. V. I. Tatarski, *Wave Propagation in Turbulent Atmosphere* (Nauka, Moscow, 1967) [in Russian].
7. J. W. Hardy, *Adaptive Optics for Astronomical Telescopes* (University Press, Oxford, England, 1998).
8. G. Lombardi, J. Navarrete, and M. Sarazin, "Review on atmospheric turbulence monitoring," *Proc. SPIE—Int. Soc. Opt. Eng.* **9148**, 91481 (2014).
9. J. Stock and G. Keller, "Astronomical seeing," *Stars Stellar Systems* **1**, 138–153 (1960).
10. M. Sarazin and F. Roddier, "The ESO differential image motion monitor," *Astron. Astrophys.* **227** (1), 294–300 (1990).
11. A. Tokovinin, "From differential image motion to seeing," *Publ. Astron. Soc. Pac.* **114**, 1156–1166 (2002).
12. A. Tokovinin and V. Kornilov, "Accurate seeing measurements with MASS and DIMM," *Mon. Not. R. Astron. Soc.* **381**, 1179–1189 (2007).
13. L. V. Antoshkin, N. N. Botygina, O. N. Emaleev, V. P. Lukin, and L. N. Lavrinova, "Differential optical meter of the parameters of atmospheric turbulence," *Atmos. Ocean. Opt.* **11** (11), 1046–1050 (1998).
14. L. V. Antoshkin, N. N. Botygina, O. N. Emaleev, P. A. Konyaev, and V. P. Lukin, "Path-averaged differential meter of atmospheric turbulence parameters," *Opt. Spectrosc.* **109** (4), 635–640 (2010).
15. J. M. Beckers, "A seeing monitor for solar and other extended object observations," *Exp. Astron.* **12**, 1–20 (2001).
16. V. Kornilov, A. Tokovinin, O. Vozyakova, A. Zaitsev, N. Shatsky, S. Potanin, and M. Sarazin, "MASS: A monitor of the vertical turbulence distribution," *Proc. SPIE—Int. Soc. Opt. Eng.* **4839**, 837–845 (2003).
17. G. R. Ochs, T.-I. Wang, R. S. Lawrence, and S. F. Clifford, "Refractive-turbulence profiles measured by one-dimensional spatial filtering of scintillations," *Appl. Opt.* **15**, 2504–2510 (1976).
18. A. A. Tokovinin, "Measurement of seeing and atmospheric time constant by differential scintillations," *Appl. Opt.* **41**, 957–964 (2002).
19. V. Kornilov, A. Tokovinin, N. Shatsky, O. Voziakova, S. Potanin, and B. Safonov, "Combined MASS-DIMM instrument for atmospheric turbulence studies," *Mon. Not. R. Astron. Soc.* **383**, 1268–1278 (2007).
20. J. Vernin and F. Roddier, "Experimental determination of two-dimensional spatiotemporal power spectra of stellar light scintillation evidence for a multilayer structure of the air turbulence in the upper troposphere," *J. Opt. Soc. Am.* **63**, 270–273 (1973).
21. A. Tokovinin, J. Vernin, A. Ziad, and M. Chun, "Optical turbulence profiles at Mauna Kea measured by MASS and SCIDAR," *Publ. Astron. Soc. Pac.* **117** (830), 395–400 (2005).
22. J. Osborn, R. W. Wilson, M. Sarazin, T. Butterley, A. Chacon, F. Derie, O. J. D. Farley, X. Haubois, D. Laidlaw, M. LeLouarn, E. Masciadri, J. Milli, J. Navarrete, and M. J. Townson, "Optical turbulence

- profiling with Stereo-SCIDAR for VLT and ELT,” *Mon. Not. R. Astron. Soc.* **478** (1), 825–834 (2018).
23. R. W. Wilson, “SLODAR: Measuring optical turbulence altitude with a Shack-Hartmann wavefront sensor,” *Mon. Not. R. Astron. Soc.* **337** (1), 103–108 (2002).
 24. T. Butterley, R. W. Wilson, M. Sarazin, C. M. Dubbel-dam, J. Osborn, and P. Clark, “Characterization of the ground layer of turbulence at Paranal using a robotic SLODAR System,” *Mon. Not. R. Astron. Soc.* **492** (1), 934–949 (2020).
 25. L. Catala, A. Ziad, Y. Fantei-Caujolle, S. M. Crawford, D. A. H. Buckley, J. Borgnino, F. Blary, M. Nickola, and T. Pickering, “High-resolution altitude profiles of the atmospheric turbulence with PML at the Sutherland Observatory,” *Mon. Not. R. Astron. Soc.* **467** (3), 3699–3711 (2017).
 26. J. Chabe, E. Aristidi, A. Ziad, H. Lanteri, Y. Fantei-Caujolle, C. Giordano, J. Borgnino, M. Marjani, and C. Renaud, “PML: A generalized monitor of atmospheric turbulence profile with high vertical resolution,” *Appl. Opt.* **59**, 7574–7584 (2020).
 27. G. B. Scharmer and T. I. M. van Werkhoven, “S-DIMM+ height characterization of day-time seeing using solar granulation,” *Astron. Astrophys.* **513**, A25 1–12 (2010).
 28. N. N. Botygina, P. G. Kovadlo, E. A. Kopylov, V. P. Lukin, M. V. Tuv, and A. Yu. Shikhovtsev, “Estimation of the astronomical seeing at the Large Solar Vacuum telescope site from optical and meteorological measurements,” *Atmos. Ocean. Opt.* **27** (2), 142–146 (2014).
 29. A. Kellerer, N. Gorceix, J. Marino, W. Cao, and P. R. Goode, “Profiles of the daytime atmospheric turbulence above Big Bear Solar Observatory,” *Astron. Astrophys.* **542**, A2 1–10 (2012).
 30. J. Kolb, R. Donaldson, J. Valenzuela, S. Oberti, B. Neichel, J. Paufique, and P.-Y. Madec, “An on-line turbulence profiler for the AOF: On-sky results,” *Proc. SPIE—Int. Soc. Opt. Eng.* **10703**, 795–802 (2018).
 31. R. Dang, Y. Yang, X.-M. Hu, Z. Wang, and S. Zhang, “A review of techniques for diagnosing the atmospheric boundary layer height (ABLH) using aerosol lidar data,” *Remote Sens.* **11** (13), 1590 (2019).
 32. A. S. Gurvich, “Lidar sounding of turbulence based on the backscatter enhancement effect,” *Izv. Atmos. Ocean. Phys.* **48** (6), 585–594 (2012).
 33. I. A. Razenkov, “Capabilities of a turbulent BSE-lidar for the study of the atmospheric boundary layer,” *Atmos. Ocean. Opt.* **34** (3), 229–238 (2021).
 34. V. V. Vorob’ev, “On the applicability of asymptotic formulas of retrieving “optical” turbulence parameters from pulse lidar sounding data: I—Equations,” *Atmos. Oceanic Opt.* **30** (2), 156–161 (2017).
 35. G. G. Gimmetstad, D. W. Roberts, J. M. Stewart, and J. W. Wood, “Development of a lidar technique for profiling optical turbulence,” *Opt. Eng.* **51** (10), 101713–101713 (2012).
 36. S. L. Odintsov, “Development and use of acoustic tools for diagnostics of the atmospheric boundary layer,” *Atmos. Ocean. Opt.* **33** (1), 104–108 (2020).
 37. A. E. Gur’yanov, B. N. Irkaev, M. A. Kallistratova, M. S. Pekur, I. V. Petenko, V. P. Ryl’kov, A. A. Semnikin, N. S. Time, E. A. Shurygin, and P. V. Shcheglov, “Complex study of optically active atmospheric turbulence in two mountain observatories,” *Astron. Zh.* **65** (3), 637–644 (1988).
 38. I. Petenko, S. Argentini, I. Pietroni, A. Viola, G. Mastrantonio, G. Casasanta, E. Aristidi, G. Bouchez, A. Agabi, and E. Bondoux, “Observations of optically active turbulence in the planetary boundary layer by sodar at the Concordia Astronomical Observatory, Dome C, Antarctica,” *Astron. Astrophys.* **568**, A44 (2014).
 39. M. Schock, S. Els, R. Riddle, W. Skidmore, T. Travouillon, R. Blum, E. Bustos, G. Chanan, S. G. Djorgovski, P. Gillett, B. Gregory, J. Nelson, A. Otarola, J. Seguel, J. Vasquez, A. Walker, D. Walker, and L. Wang, “Thirty meter telescope site testing. I: Overview,” *Publ. Astron. Soc. Pac.* **121** (878), 384–395 (2009).
 40. A. A. Tikhomirov, “Ultrasonic anemometers and thermometers for measuring fluctuations of air flux velocity and temperature. Review,” *Opt. Atmos. Okeana* **23** (7), 585–600 (2010).
 41. E. Aristidi, J. Vernin, E. Fossat, F.-X. Schmider, T. Travouillon, C. Pouzenc, O. Traulle, C. Genthon, A. Agabi, E. Bondoux, Z. Challita, D. Mekarnia, F. Jeanneaux, and G. Bouchez, “Monitoring the optical turbulence in the surface layer at Dome C, Antarctica, with sonic anemometers,” *Mon. Not. R. Astron. Soc.* **454** (4), 4304–4315 (2015).
 42. V. P. Lukin, N. N. Botygina, O. N. Emaleev, L. V. Antoshkin, P. A. Konyaev, V. A. Gladkikh, V. P. Mamysh, and S. L. Odintsov, “Simultaneous measurements of structure characteristics of atmospheric refraction by optical and acoustic methods,” *Atmos. Ocean. Opt.* **25** (1), 6–11 (2012).
 43. V. P. Lukin, N. N. Botygina, V. A. Gladkikh, O. N. Emaleev, P. A. Konyaev, S. L. Odintsov, and A. V. Torgaev, “Joint measurements of atmospheric turbulence level with optical and acoustic meters,” *Atmos. Ocean. Opt.* **28** (3), 254–257 (2015).
 44. Y. H. Ono, Y. Minowa, O. Guyon, C. S. Clergeon, E. Mieda, J. Lozi, T. Hattori, and M. Akiyama, “Overview of AO Activities at Subaru Telescope,” *Proc. SPIE—Int. Soc. Opt. Eng.* **11448**, 114480 (2020).
 45. J. C. Christou, C. Veillet, D. Miller, G. Brusa, A. Cavallaro, G. Taylor, L. Funk, A. Conrad, G. Rahmer, X. Zhang, S. Walsh, S. Ertel, E. Pinna, and S. Esposito, “Adaptive optics all the time at the LBTO,” *Proc. SPIE—Int. Soc. Opt. Eng.* **11448**, 1144824 (2020).
 46. S. Hippler, W. Brandner, S. Scheithauer, M. Kulas, J. Panduro, P. Bizenberger, H. Bonnet, C. Deen, F. Delplancke-Strobele, F. Eisenhauer, G. Finger, Z. Hubert, J. Kolb, E. Muller, L. Pallanca, J. Woillez, and G. Zins, “Infrared wavefront sensing for adaptive optics assisted galactic center observations with GRAVITY,” *Proc. SPIE—Int. Soc. Opt. Eng.* **11448**, 114484 (2020).
 47. F. Patru, F. Millour, O. Lai, M. Carillet, F. Eisenhauer, S. Gillessen, M. Haase, M. Hart, F. Haussmann, J.-B. Le Bouquin, D. Lutz, C. Mandla, N. More, T. Ott, T. Paumard, C. Rau, J. Schubert, E. Wieprecht, J. Woillez, and S. Yazici, “Dimensioning adaptive optics for future VLTI projects,” *Proc. SPIE—Int. Soc. Opt. Eng.* **11448**, 1144871 (2020).
 48. S. C. Chapman, U. Conod, P. Turri, K. Jackson, O. Lardiere, S. Sivanandam, D. Andersen, C. Correia, M. Lamb, C. Ross, G. Sivo, and J.-P. Veran, “The

- multi-object adaptive optics system for the Gemini infra-red multi-object spectrograph,” *Proc. SPIE—Int. Soc. Opt. Eng.* **11448**, 1144872 (2020).
49. U. Conod, K. Jackson, O. Lardiere, S. Chapman, P. Turri, M. Lamb, S. Sivanandam, G. Sivo, and J.-P. Veran, “Developing the prototype adaptive optics system for the Gemini infra-red multi-object spectrograph,” *Proc. SPIE—Int. Soc. Opt. Eng.* **11448**, 1144876 (2020).
 50. P. Ciliegi, G. Agapito, M. Aliverti, and C. Arcidiacono, “MAORY: The adaptive optics module for the Extremely Large Telescope (ELT),” *Proc. SPIE—Int. Soc. Opt. Eng.* **11448**, 114480 (2020).
 51. A. D. Hedglen, L. M. Close, A. H. Bouchez, J. R. Males, R. Demers, M. Kautz, R. Basant, M. Parkinson, V. Gasho, F. Quiros-Pacheco, and B. N. Sitariski, “The Giant Magellan Telescope high contrast phasing testbed,” *Proc. SPIE—Int. Soc. Opt. Eng.* **11448**, 114482 (2020).
 52. A. Tokovinin, S. Baumont, and J. Vasquez, “Statistics of turbulence profile at Cerro Tololo,” *Mon. Not. R. Astron. Soc.* **340** (1), 52–58 (2003).
 53. L. J. Sanchez, I. Cruz-Gonzalez, J. Echevarria, A. Ruelas-Mayorga, A. M. Garcia, R. Avila, E. Carrasco, A. Carraminana, and A. Nigoche-Netro, “Astroclimate at San Pedro Martir—I. seeing statistics between 2004 and 2008 from the thirty meter telescope site-testing data,” *Mon. Not. R. Astron. Soc.* **426**, 635–646 (2012).
 54. L. C. Roberts and L. W. Bradford, “Improved models of upper-level wind for several astronomical observatories,” *Opt. Express* **19**, 820–837 (2011).
 55. P. Haguenaer, A. Guesalaga, and T. Butterley, “Comparison of atmosphere profilers at Paranal and atmosphere parameters statistics: AOF-profiler, STEREO-SCIDAR, MASS-DIMM, LGS-WFS,” *Proc. SPIE—Int. Soc. Opt. Eng.* **11448**, 114. Cited January 28, 2021.
 56. URL: <https://www.eso.org/public/industry/cp/docs/CFT-advance.html> (last access: 28.01.2021).
 57. J. Milli, T. Rojas, B. Courtney-Barrer, F. Bian, J. Navarrete, F. Kerber, and A. Otarola, “Turbulence nowcast for the Cerro Paranal and Cerro Armazones Observatory sites,” *Proc. SPIE—Int. Soc. Opt. Eng.* **11448**, 114481 (2020).
 58. A. Turchi, E. Masciadri, and L. Fini, “Forecasting surface-layer atmospheric parameters at the Large Binocular Telescope site,” *Mon. Not. R. Astron. Soc.* **466** (2), 1925–1943 (2017).
 59. E. Masciadri and L. Fini, “Forecast of surface layer meteorological parameters at Cerro Paranal with a mesoscale atmospheric model,” *Mon. Not. R. Astron. Soc.* **449**, 1664–1678 (2015).
 60. J. Osborn and M. Sarazin, “Atmospheric turbulence forecasting with a general circulation model for Cerro Paranal,” *Mon. Not. R. Astron. Soc.* **480** (1), 1278–1299 (2018).
 61. R. Lyman, T. Cherubini, and S. Businger, “Forecasting seeing for the Maunakea Observatories,” *Mon. Not. R. Astron. Soc.* **496** (4), 4734–4748 (2020).
 62. C. Qing, X. Wu, X. Li, T. Luo, C. Su, and W. Zhu, “Mesoscale optical turbulence simulations above Tibetan Plateau: First attempt,” *Opt. Express* **28**, 4571–4586 (2020).
 63. E. Masciadri, G. Martelloni, and A. Turchi, “Filtering techniques to enhance optical turbulence forecast performances at short time-scales,” *Mon. Not. R. Astron. Soc.* **492**, 140–152 (2020).
 64. C. Qing, X. Wu, H. Huang, Q. Tian, W. Zhu, R. Rao, and X. Li, “Estimating the surface layer refractive index structure constant over snow and sea ice using Monin–Obukhov similarity theory with a mesoscale atmospheric model,” *Opt. Express* **24**, 20424–20436 (2016).
 65. Y. Wang and S. Basu, “Using an artificial neural network approach to estimate surface-layer optical turbulence at Mauna Loa, Hawaii,” *Opt. Lett.* **41**, 2334–2337 (2016).
 66. C. Jellen, J. Burkhardt, C. Brownell, and C. Nelson, “Machine learning informed predictor importance measures of environmental parameters in maritime optical turbulence,” *Appl. Opt.* **59**, 6379–6389 (2020).
 67. C. Su, X. Wu, T. Luo, S. Wu, and C. Qing, “Adaptive niche-genetic algorithm based on back propagation neural network for atmospheric turbulence forecasting,” *Appl. Opt.* **59**, 3699–3705 (2020).
 68. V. P. Lukin, B. V. Fortes, L. V. Antoshkin, N. N. Botygina, O. N. Emaleev, L. N. Lavrinova, A. I. Petrov, A. P. Yankov, A. V. Bulatov, P. G. Kovadlo, and N. M. Firstova, “Experimental setup of adaptive optical system for LSVT. I. Testing results and perspectives,” *Atmos. Ocean. Opt.* **12** (12), 1107–1110 (1999).
 69. V. P. Lukin, V. M. Grigorjev, L. V. Antoshkin, N. N. Botygina, O. N. Emaleev, P. A. Konyaev, E. A. Kopylov, V. V. Lavrinov, P. G. Kovadlo, and V. I. Skomorovskii, “Tests of the adaptive optical system with a modified correlation sensor at the big solar vacuum telescope,” *Atmos. Ocean. Opt.* **20** (5), 379–386 (2007).
 70. V. P. Lukin, N. N. Botygina, L. V. Antoshkin, A. G. Borzilov, O. N. Emaleev, P. A. Konyaev, P. G. Kovadlo, D. Yu. Kolobov, A. A. Selin, E. L. Soin, A. Yu. Shikhovtsev, and S. A. Chuprakov, “Multi-cascade image correction system for the Large Solar Vacuum Telescope,” *Atmos. Ocean. Opt.* **32** (5), 597–606 (2019).
 71. P. V. Shcheglov and A. E. Gur’yanov, “About astronomical quality of astronomical imagery at certain sites in USSR,” *Astron. Zh.* **68** (3), 632–638 (1991).
 72. P. V. Shcheglov, *Optical Astronomy Problems* (Nauka, Moscow, 1980) [in Russian].
 73. Sh. P. Darchiya, *Astronomical Climate of USSR* (Nauka, Moscow, 1985) [in Russian].
 74. B. Garcia-Lorenzo, J. J. Fuensalida, C. Munoz-Tunon, and E. Mendizabal, “Astronomical site ranking based on tropospheric wind statistics,” *Mon. Not. R. Astron. Soc.* **356**, 849–858 (2005).
 75. S. Chueca, B. Garcia-Lorenzo, C. Munoz-Tunon, and J. J. Fuensalida, “Statistics and analysis of high-altitude wind above the Canary Islands observatories,” *Mon. Not. R. Astron. Soc.* **349**, 627–631 (2004).
 76. E. Carrasco, R. Avila, and A. Carramin, “High-altitude wind velocity at Sierra Negra and San Pedro Martir,” *Publ. Astron. Soc. Pac.* **117**, 104–110 (2005).
 77. B. Garcia-Lorenzo, A. Eff-Darwich, J. J. Fuensalida, and J. Castro-Almazan, “Adaptive optics parameters connection to wind speed at the Teide Observatory,” *Mon. Not. R. Astron. Soc.* **397**, 1633–1646 (2009).

78. Y. Hach, A. Jabiri, A. Ziad, A. Bounhir, M. Sabil, A. Abahamid, and Z. Benkhaldoun, "Meteorological profiles and optical turbulence in the free atmosphere with NCEP/NCAR data at Oukaimeden—I. Meteorological parameters analysis and tropospheric wind regimes," *Mon. Not. R. Astron. Soc.* **420** (1), 637–650 (2012).
79. http://iac.es/proyecto/site-testing/images/stories/pdf/varela_et_al_2012.pdf. Cited January 28, 2021.
80. L. A. Bolbasova, A. Yu. Shikhovtsev, E. A. Kopylov, A. A. Selin, V. P. Lukin, and P. G. Kovadlo, "Daytime optical turbulence and wind speed distributions at the Baikal Astrophysical Observatory," *Mon. Not. R. Astron. Soc.* **482** (2), 2619–2626 (2019).
81. J. A. Hellemeier, R. Yang, M. Sarazin, and P. Hickson, "Weather at selected astronomical sites—an overview of five atmospheric parameters," *Mon. Not. R. Astron. Soc.* **482** (4), 4941–4950 (2019).
82. J. C. Marín, D. Pozo, and M. Cur é, "Estimating and forecasting the precipitable water vapor from GOES satellite data at high altitude sites," *Astron. Astrophys.* **573**, A41 (2015).
83. A. Yu. Shikhovtsev, P. G. Kovadlo, and A. V. Kiselev, "Astroclimatic statistics at the Sayan Solar Observatory," *Sol.-Terr. Phys.* **6** (1), 102–107 (2020).
84. A. Yu. Shikhovtsev, L. A. Bolbasova, P. G. Kovadlo, and A. V. Kiselev, "Atmospheric parameters at the 6-m Big Telescope Alt-Azimuthal Site," *Mon. Not. R. Astron. Soc.* **493** (1), 723–729 (2020).
85. V. Kornilov, N. Shatsky, O. Voziakova, B. Safonov, S. Potanin, and M. Kornilov, "First results of a site-testing programme at Mount Shatdzhatmaz during 2007–2009," *Mon. Not. R. Astron. Soc.* **408** (2), 1233–1248 (2010).
86. V. Kornilov, B. Safonov, M. Kornilov, N. Shatsky, O. Voziakova, S. Potanin, I. Gorbunov, V. Senik, and D. Cheryasov, "Study on atmospheric optical turbulence above Mount Shatdzhatmaz in 2007–2013," *Publ. Astron. Soc. Pac.* **126** (939), 482–495 (2014).
87. A. Yu. Shikhovtsev, Avtoref. Candidate's Dissertation in Mathematics and Physics (Institute of Solar-Terrestrial Physics SB RAS, Irkutsk, 2016).
88. P. G. Kovadlo, V. P. Lukin, and A. Yu. Shikhovtsev, "Development of the model of turbulent atmosphere at the Large Solar Vacuum Telescope site as applied to image adaptation," *Atmos. Ocean. Opt.* **32** (2), 202–206 (2019).
89. A. Shikhovtsev, P. Kovadlo, V. Lukin, V. Nosov, A. Kiselev, D. Kolobov, E. Kopylov, M. Shikhovtsev, and F. Avdeev, "Statistics of the optical turbulence from the micrometeorological measurements at the Baikal Astrophysical Observatory site," *Atmosphere* **10**, 661–1 (2019).
90. V. V. Nosov, V. P. Lukin, E. V. Nosov, and A. V. Torgaev, "Turbulence scales of the Monin–Obukhov similarity theory in the anisotropic mountain boundary layer," *Rus. Phys. J.* **63** (2), 244–249 (2020).
91. V. Nosov, V. Lukin, E. Nosov, A. Torgaev, and A. Bogushevich, "Measurement of atmospheric turbulence characteristics by the ultrasonic anemometers and the calibration processes," *Atmosphere* **10** (8), 460–1 (2019).
92. V. V. Nosov, P. G. Kovadlo, V. P. Lukin, and A. V. Torgaev, "Atmospheric coherent turbulence," *Atmos. Ocean. Opt.* **26** (3), 201–206 (2013).
93. V. V. Nosov, V. M. Grigor'ev, P. G. Kovadlo, V. P. Lukin, E. V. Nosov, and A. V. Torgaev, "Recommendations for the site selection of sites for the ground-based astronomical telescopes," *Opt. Atmos. Okeana* **23** (12), 1099–1110 (2010).
94. V. P. Lukin, E. V. Nosov, V. V. Nosov, and A. V. Torgaev, "Causes of non-Kolmogorov turbulence in the atmosphere," *Appl. Opt.* **55**, B163–B168 (2016).
95. V. V. Nosov, V. P. Lukin, E. V. Nosov, A. V. Torgaev, V. L. Afanas'ev, Yu. U. Balega, V. V. Vlasjuk, V. E. Panchuk, and G. V. Yakopov, "Astroclimate studies in the Special Astrophysical Observatory of the Russian Academy of Sciences," *Atmos. Ocean. Opt.* **32** (1), 8–18 (2019).
96. V. V. Nosov, V. P. Lukin, P. G. Kovadlo, E. V. Nosov, and A. V. Torgaev, *Optical Properties of Turbulence in the Mountain Boundary Air Layer* (Publishing House of SB RAS, Novosibirsk, 2016) [in Russian].
97. V. V. Nosov, V. P. Lukin, E. V. Nosov, and A. V. Torgaev, "Formation of turbulence at astronomical observatories in Southern Siberia and North Caucasus," *Atmos. Ocean. Opt.* **32** (4), 464–482 (2019).
98. N. N. Peretyatk, "Study of astroclimate at Terskol Peak," *Kinemat. Fiz. Nebesnykh Tel* **16** (5), 470–476 (2000).
99. F. Cantalloube, J. Milli, C. Bohm, S. Crewell, J. Navarrete, K. Rehfeld, M. Sarazin, and A. Sommani, "The impact of climate change on astronomical observations," *Nature Astron.* **4**, 826–829 (2020).

Translated by O. Ponomareva